

# On the Source of Energetic Electron Precipitation during Auroral Substorms

Nithin Sivadas, Michael Hirsch, Toshi Nishimura, Joshua L. Semeter

Centre for Space Physics and Department of Electrical and Computer Engineering, Boston University

Contact: [nithin@bu.edu](mailto:nithin@bu.edu)

## 1. Abstract

Precipitating auroral electrons are believed to originate mainly from parallel electric fields set up at the auroral acceleration region (AAR) extending up to 20,000 km altitude. However, electrons of energy greater than 100 keV are probably generated by acceleration processes beyond the AAR. Observational evidence for the source location of these energetic electrons are hard to come by. In our current work, we present simultaneous magnetically conjugate measurements of energetic electron spectra estimated at the ionosphere using the Poker Flat Incoherent Scatter Radar (PFISR) and measured at the inner plasma sheet by the THEMIS spacecraft. The flux of precipitating electrons of energy greater than 100 keV demonstrate a striking spatio-temporal correlation with that of the inner plasma sheet electrons. This suggests that the source of the energetic electrons lie at or beyond the inner plasma sheet, and that the acceleration processes within the auroral acceleration zone don't contribute substantially to their energization. Using simultaneous THEMIS measurements of wave power, we speculate that the electromagnetic ion cyclotron (EMIC) and Chorus waves are likely candidates for electron acceleration within the inner plasma sheet apart from the usual candidates of betatron and fermi acceleration. However, between the ionosphere and the plasma sheet, electrons of energy less than 100 keV show significant differences in their energy spectra after the substorm onset suggesting an active AAR.

## 2. Magnetospheric Substorms

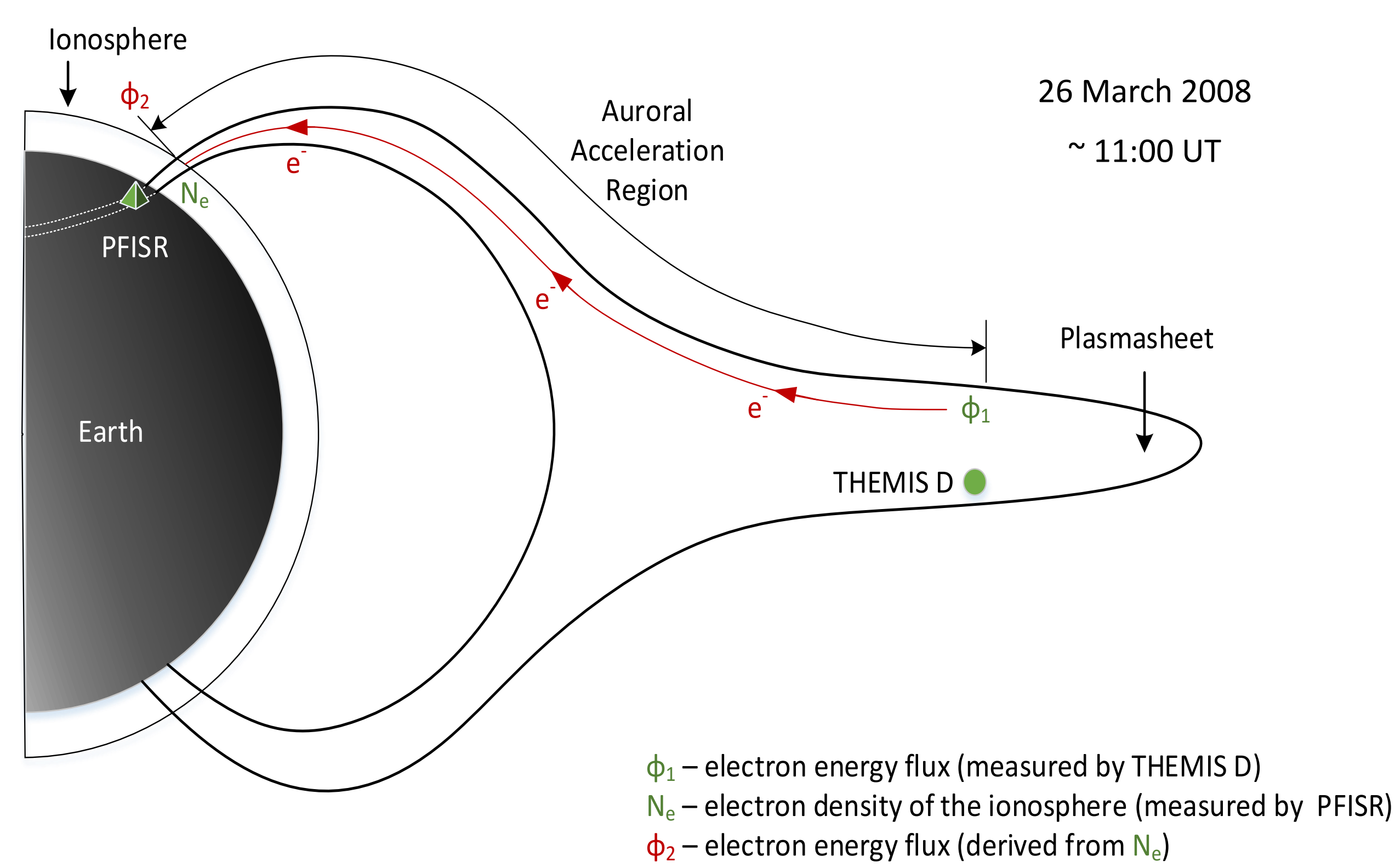


**Figure 1:** The relative positions of the measurements and derived quantities presented in this poster. Measured—Green; Derived — Red

A magnetospheric substorm is an energy storage—release process which develops through the following steps:

- Growth** : Energy is stored in the magnetotail from the solar wind
- Substorm onset** : It is then released by a large-scale instability within the magneto-tail
- Expansion** : The energy is dissipated in the magnetosphere-ionosphere system
- Recovery** : Finally, the system returns to a quiet state

In this poster, we describe a substorm event observed by THEMIS-D Spacecraft  $\sim 1 R_E$  south of the neutral sheet. Simultaneously, magnetically conjugate observations of electron density enhancements in the ionosphere were being made by the Poker Flat Incoherent Scatter Radar (PFISR). We compare the electron energy spectra measured by THEMIS-D in the plasma-sheet ( $\phi_1$ ) with the precipitated electron energy spectra in the ionosphere ( $\phi_2$ ) derived from PFISR electron density measurements ( $N_e$ ) and discuss its implications.

## 3. Plasma-sheet during a Substorm Event

- Plasma-sheet is a region of higher-density plasma that lies between the two tail lobes of the magnetosphere
- Increase in magnetic flux in the tail during the growth phase, results in the thinning of the plasma sheet (See time  $t_2$  in figure 2) [1]
- During the onset, the stored magnetotail energy is released through reconnection of the closed plasma-sheet field lines. The field lines contract earthward due to their magnetic tension, and become more dipolar as they travel earthward. (See time  $t_3$  in figure 2)

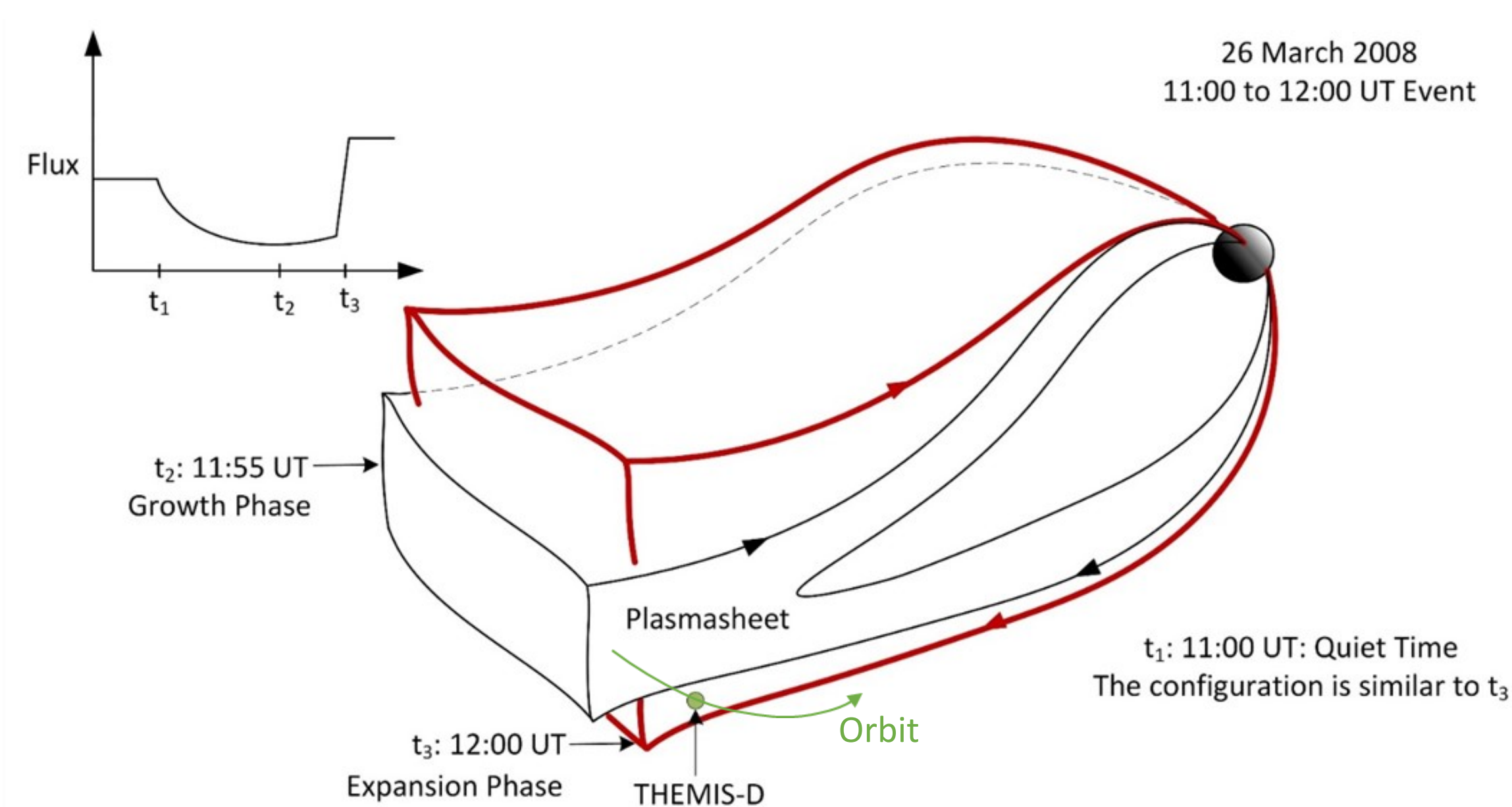


**Figure 2:** Plasma-sheet thinning and expanding before and after the substorm onset.

## 3. Ionosphere during a Substorm Event

- During the growth phase, electron precipitation of up to 100 keV were observed to be moving equatorward along with the auroral arc
- At the onset, poleward motion of the electron precipitation up to 300 keV were observed correlated with the plasma sheet expansion

**3.1 Using Incoherent Scatter Radar (ISR) to measure Energy Spectra of Precipitating Electrons** Using altitude profiles of electron density (measured by ISRs), and a suitable model for the neutral atmospheric density, and ion chemistry in the ionosphere, we derived the energy spectra of precipitating primary electrons as follows:

- Production rates ( $q$ ) were calculated from the measured electron density ( $N_e$ ) by assuming an effective recombination coefficient ( $\alpha_{eff}$ )

$$q = \frac{dN_e}{dt} + \alpha_{eff} N_e^2$$

- A numerical model [2] is used to compute the production rate ( $q$ ) profiles for a discrete set of monoenergetic electron beams. The computed profiles represent a discrete forward model A relating an incident electron flux spectrum to a corresponding altitude profile of production rates (See figure 5).

$$q = [A] \phi_2$$

- Finally, the electron energy flux spectrum is derived by inverting the matrix A to arrive at a discrete estimate of the differential number flux spectrum. Here we use the maximum entropy method to invert the matrix, as described in [3].

$$\phi_2 = inv[A] \left( \frac{dN_e}{dt} + \alpha_{eff} N_e^2 \right)$$

## 4. Magnetically Conjugate Measurements

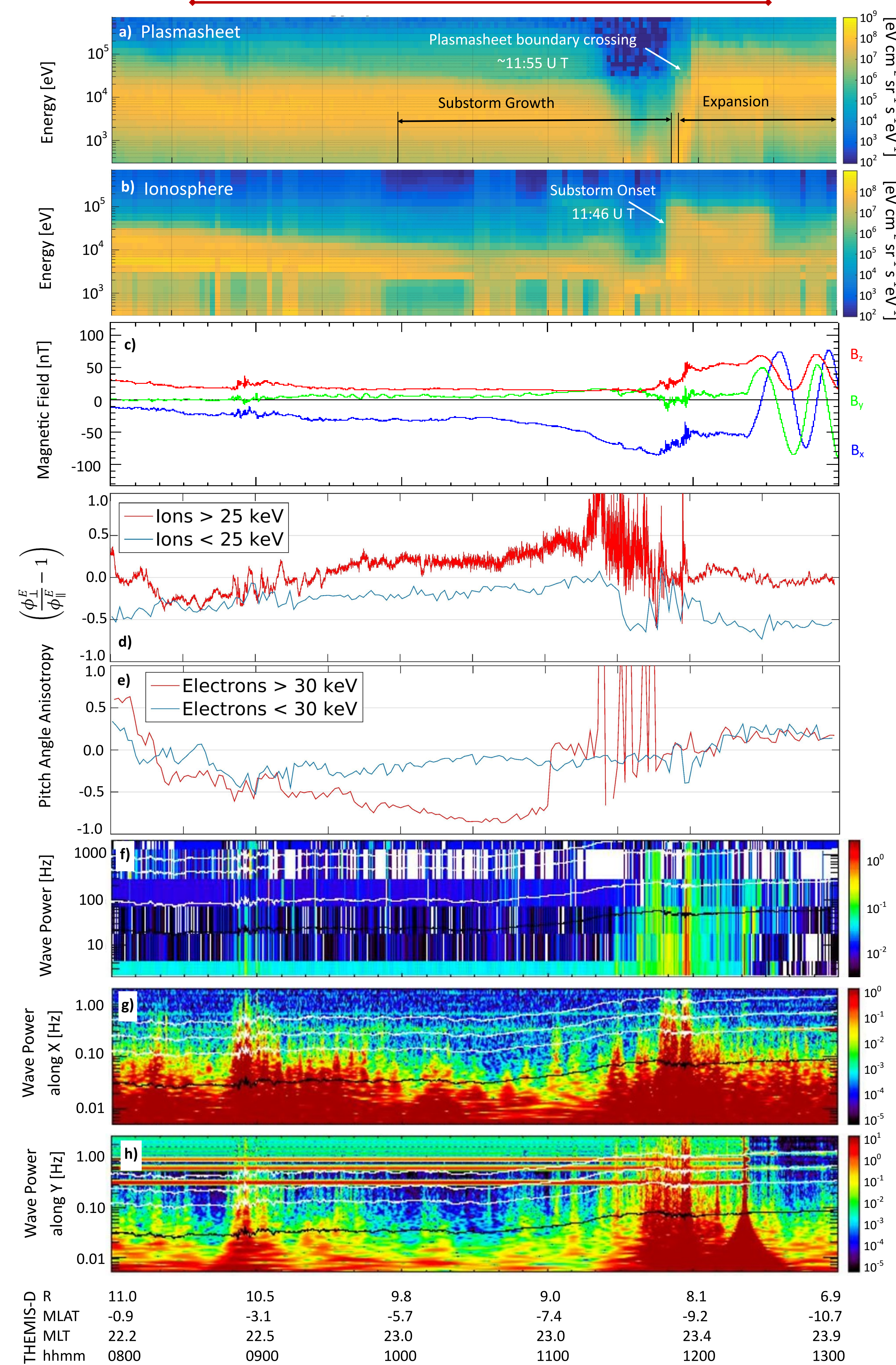


**Figure 3:** Energy spectra: a) of electrons measured by THEMIS-D in the plasma sheet and b) of precipitated electrons estimated by PFISR at the ionosphere; c) magnetic field in GSM coordinates; d) ion anisotropy; e) electron anisotropy; f) wave power for frequencies 1 to 1000 Hz; g) wave power along GSM-X coordinate; h) wave power along GSM-Y coordinate. b) was estimated from the ground, the rest are measured by THEMIS-D.

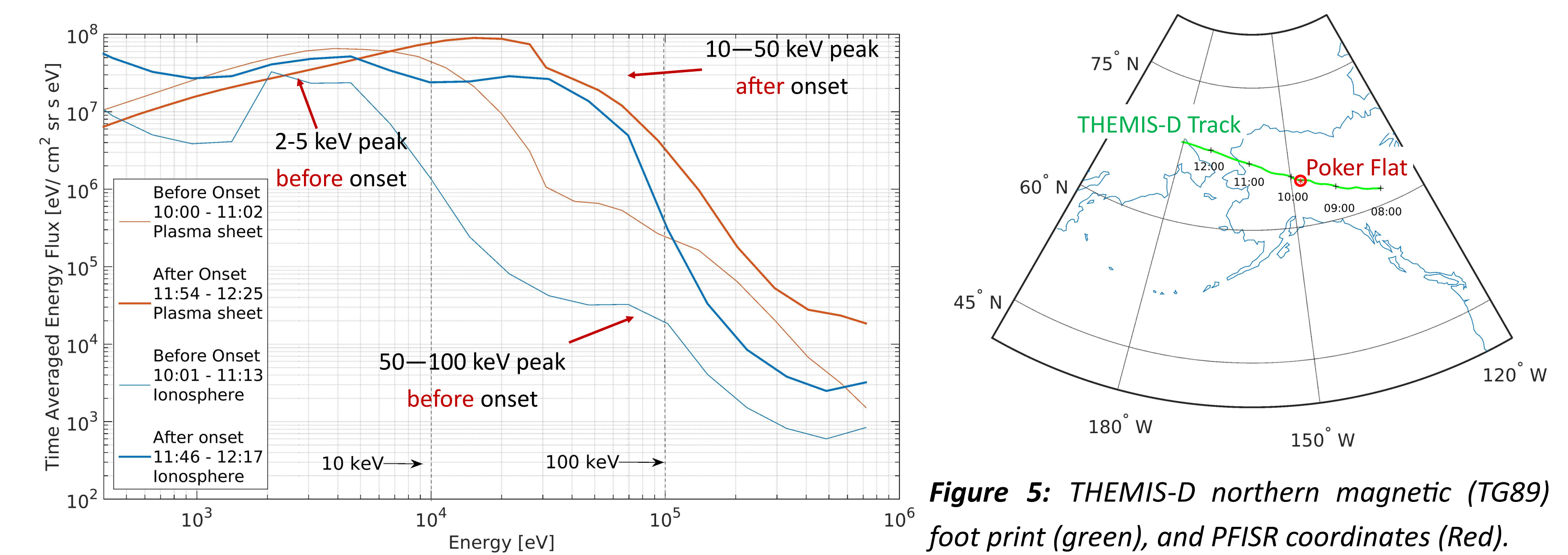


**Figure 4:** Time averaged energy spectra before and after the onset at the plasma sheet and ionosphere.

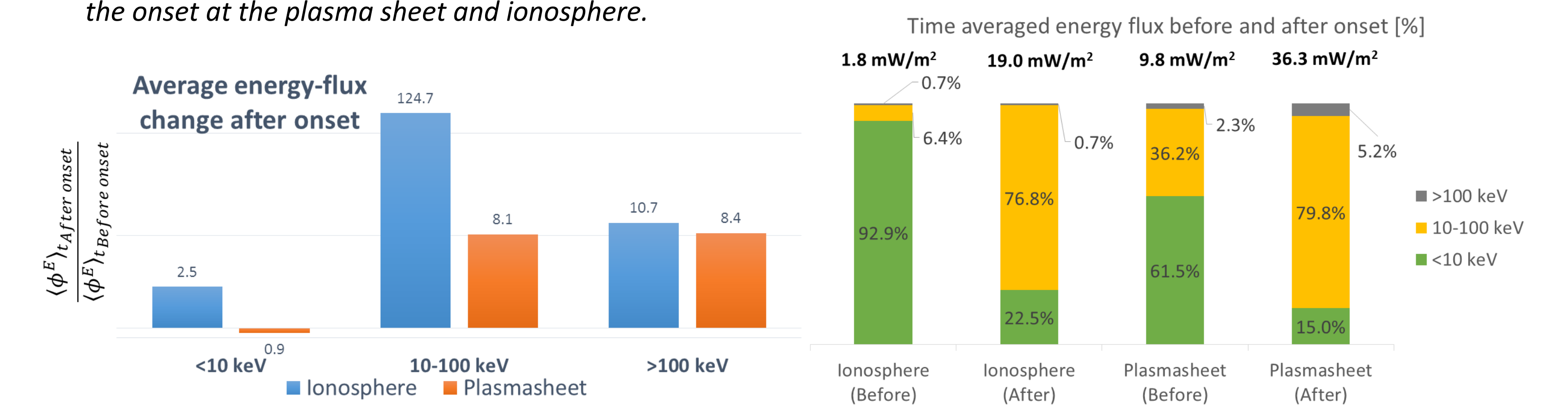


**Figure 6:** Relative change in the average energy flux, before and after the onset at the ionosphere and plasmasheet

**Figure 7:** Relative kinetic power of electrons in different energy bins, before & after the onset in the ionosphere and plasmasheet

## 5. Discussion

**Correlated electron energy spectra:** Figure 3 a & b, demonstrate a broad correlation between the variation of electron energy spectra in the plasma sheet and the ionosphere. The depletion of flux at  $\sim 11:30$  UT, is due to the thinning of the plasma sheet and corresponding equatorward motion of the plasma sheet's ionospheric foot print.

**Evidence of plasma sheet thinning:** The  $B_x$  (earthward) and  $B_z$  (along magnetic dipole) field values, in Figure 3 c, suggest the thinning of the plasma sheet during growth phase, and sudden dipolarization after the onset.

**Betatron & Fermi Acceleration:** During dipolarization, as the plasma moves earthward,  $B_x$  increases ( $\Rightarrow$  betatron) and the length of the magnetic field line decreases ( $\Rightarrow$  fermi). (See corresponding increase in the electron anisotropy, perpendicular energy flux, after the substorm onset in Figure 3 e.)

**Betatron:** Energization  $\propto B_x$  (acts mainly on particles with pitch angles near  $90^\circ$ )

**Fermi:** Energization  $\propto B_x^{2/5}$  (acts mainly on particles with low pitch angles) [4]

**Chorus Waves:** They are mostly not observed, except at the onset time. During the onset chorus could contribute towards the scattering and energization of electrons with energy < 30 keV.

**EMIC Waves:** They are low frequency waves (0.01 ~ 5 Hz), usually found outside the plasmasphere. Figure 3 g, h show a significant presence of EMIC waves in the inner plasma sheet through all the phases of the substorm. They are produced by plasma instability due to a positive ion anisotropy in Figure 3 d. EMIC wave can undergo bounce resonance with electrons of energy 0.1 to 100 keV, and cause pitch angle scatter or even acceleration. They act predominantly on equatorially mirroring electrons. [5]

**Energetic precipitation during growth phase:** The energy spectra during the growth phase peaks at around 2-5 keV and 50-100 keV at both the plasmasheet and the ionosphere. Moreover, the difference in the energy spectra of the precipitating electrons on the ionosphere, and that observed at the plasmasheet appear to be only a scaling factor.  $\Rightarrow$  The AAR plays a minimal role in altering the energy spectra of the precipitating electrons, and the source lies at or tailward of the inner-plasmasheet. [6]

**Energetic precipitation during the expansion phase:** The energy spectra at both the ionosphere and plasmasheet peak between 10-50 keV. However, from Figure 6, we observe a marked decrease in the energy flux of electrons < 10 keV in the plasma sheet, suggesting acceleration to higher energies. The substantial difference between the ionosphere and plasmasheet electron energy spectra, specifically for energies < 100 keV, suggest an active AAR that energizes cold electrons up to 100 keV. Electrons > 100 keV demonstrate a striking correlation in Figure 4, and Figure 6, and are likely caused by reconnection at the magnetotail.

**Significant energetic electron precipitation (10-100keV) after the onset:** Figure 7, shows that a significant contribution of the power after the substorm onset in the plasmasheet and ionosphere is from electrons of energy ranging from 10-100 keV.

## 6. Conclusion

- ISR measurements offer a rich description of electrons within the loss cone
- Combined with spacecraft measurements in the plasmasheet they provide insights into the relative significance of source regions and acceleration mechanisms
- Precipitating electrons > 100 keV likely originate at or tailward of the inner-plasmasheet
- Precipitating electrons from 10-100 keV are mostly energized by the AAR after the onset. However, they likely originate from the inner-plasmasheet or tailward of it during the growth phase.
- Precipitating electrons < 10 keV seem to be mostly produced by the AAR, especially after the substorm onset. However, during the growth phase, their source might still be the plasmasheet.
- Growth phase energetic precipitation, observed by ISRs, may be used as a short-term precursor for large substorms.

### References:

- [1] Arford, W. L., Pletschek, H. E., and Siscoe, G. L.: Tail of the magnetosphere, *J. Geophys. Res.*, 70, 1231-1236, 1965.
- [2] Sergiyenko, T. I., Ivanov, V. E.: A new approach to calculate the excitation of atmospheric gases by auroral electron impact, *Ann. Geophysica*, 11, 717-727, 1993.
- [3] Semeter, J., and F. Kamalabadi (2005), Determination of primary electron spectra from incoherent scatter radar measurements of the auroral E region, *Radio Sci.*, 40, RS2006.
- [4] Brin, J., Artemyev, A. V., Baker, D. N., Echlin, M., Hoshino, M., Zelenyi, L. M.: Particle Acceleration in the Magnetotail and Aurora, *Space Sci. Rev.*, 173, 49-102, 2012.
- [5] Shprits, Y. Y.: Potential waves for pitch-angle scattering of near-equatorially mirroring energetic electrons due to violation of the second adiabatic invariant, *Geo. Res. Lett.*, 36, 200
- [6] Pytte, T., West, H. I.: Ground-satellite correlations during presubstorm magnetic field configuration changes and plasma sheet thinning in the near-Earth magnetotail, *Journal of Geo. Res.*, 83, A8, 3791-3804, 1978

**Acknowledgements:** We thank John Swoboda, for his work on developing the GeoData tool—<https://github.com/jswoboda/GeoDataMATLAB>, which we have extensively used to work with PFISR measurements.